

5.3. Amundsen-Scott South Pole Station (1/25/07–1/17/08)

The 2007–2008 season at Amundsen-Scott South Pole Station is defined as the period between system inspection on 1/24/07–1/25/07 and the site visit on 1/17/08–1/24/08. Season opening and closing calibrations were performed on 1/24/07–1/25/07 and 1/17/08–1/18/08, respectively. Volume 17 solar data comprise the period 1/25/07–1/17/08. A total of 16995 scans are part of the South Pole Volume 17 dataset.

The SUV-100 spectroradiometer worked almost flawlessly during the reporting period (only 8 scans were missed due to technical problems), but the performance of the ancillary sensors was affected by several issues:

- The 305, 313, and 320 nm channels of the GUV-541 radiometer suffered from an unusually large change in sensitivity by 6%, 5%, and 14%, respectively. These drifts were corrected by adjusting the channel's calibration factors accordingly. The uncertainty of the measurements is increased by about $\pm 2\%$.
- Solar data indicate that the calibration of the Eppley TUVR radiometer has increased by 16% during 2007. The calibration of the instrument was not adjusted. Data from TUVR should be treated as if they were uncalibrated and only be used for assessments of short-term variations.
- The receiving surface of the Eppley PSP pyranometer was not parallel to its outer rim that is used for leveling. This deficiency was corrected by slightly tilting the instrument. However, some systematic errors remain in solar data and manifest themselves as a sinusoidal variation with a period of one day and an amplitude of about 2%.

5.3.1. Irradiance Calibration

The on-site standards of irradiance for the 2007/08 season were the lamps 200W021 and M-666. A third on-site standard, lamp 200W006, became unstable in December 2006 and was not used for the calibration of solar data. Lamp 200W017 served as traveling standard at the beginning of the season. This lamp was calibrated by Optronic Laboratories in March 2001. Lamp M-763 was the traveling standard at the site visit in 2008. It has been calibrated in July 2007 at BSI with a set of four 1000-W FEL lamps, which had been calibrated by the U.S. Central UV Calibration Facility (CUCF) in Boulder, Colo. The bulb of lamp M-763 was slightly rotated in its holder sometime in October. Comparisons with other lamps before and after the misalignment indicated that the rotation changed the irradiance of lamp M-763 by about 2% in the UV and 1-2% in the visible. The effect of the misalignment was adjusted by applying a correction function to the calibration values of the lamp.

The original calibration of lamp 200W021 was established by Optronic Laboratories in September 1998. Lamp M-666 was originally calibrated with lamps 200W006 and 200W021, using season closing scans of Volume 9 and opening scans of Volume 10.

Based on comparisons performed during the site visit in January 2006, it was determined that lamps 200W021 and M-666 had drifted by about 2%. New calibration were transferred to the lamp using the traveling standard 200W017 as reference, and these calibrations were also used to process solar data from the 2007/08 season. Details of the calibration transfer are provided in the Volume 15 Operations Report.

Figure 5.3.1 shows a comparison at the start of the season (1/24/07-1/25/07). The calibrations of lamps 200W021 and M-666 agreed with that of lamp 200W017 to within $\pm 1\%$. The calibration of lamp 200W006 was different by 3.5% and exhibited instabilities for wavelengths above 500 nm, confirming the lamp's demise. Figure 5.3.2 shows the comparison of lamps 200W021 and M-666 with M-763 at the end of the reporting period. The calibration of both site standard agreed with M-763 to within $\pm 1.5\%$. The lamps were

again compared a few days later as part of the “opening calibrations” for Volume 18 data. Results of this comparison are shown in Figure 5.3.3. The calibration of both site standard agreed with lamp M-763 to within $\pm 1.0\%$. A comparison of Figure 5.3.1 - 5.3.3 confirms that the Optronic Laboratory calibration from 2001 preserved by lamp 200W017 is consistent with the CUCF-based calibration of lamp M-763 from 2007 to within the expected uncertainty of lamp transfers ($\pm 1\%$) and the rotation-correction of M-763.

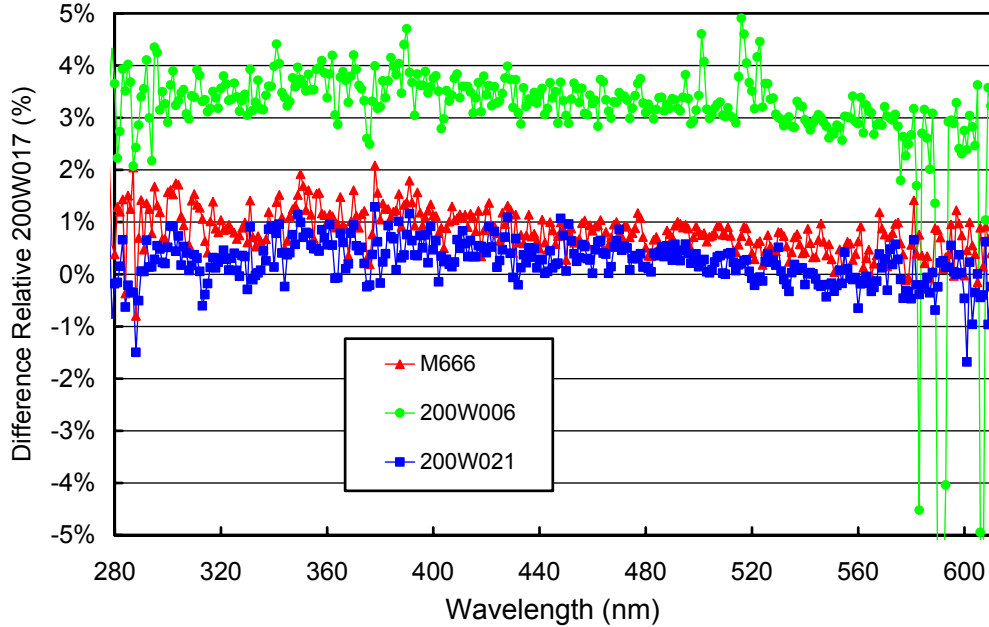


Figure 5.3.1. Comparison of South Pole lamps 200W006, 200W021, and M-666 with BSI traveling standard 200W017 at the beginning of the season (1/24/07–1/25/07).

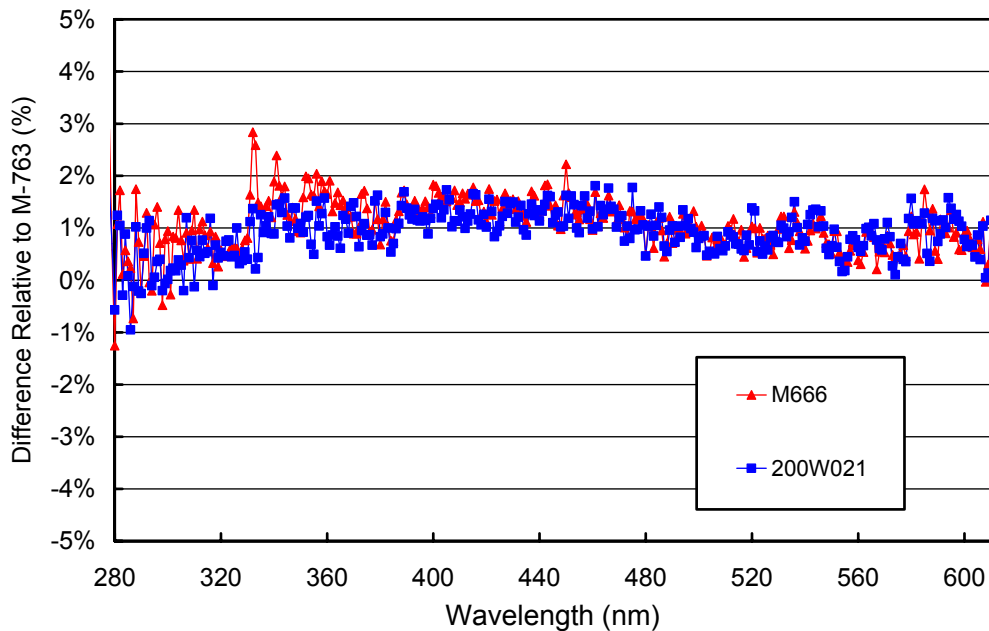


Figure 5.3.2. Comparison of South Pole lamps 200W021, and M-666 with BSI traveling standard M-763 at the end of the season (1/17/08–1/18/08). Data of lamp M-763 have been corrected for the effect of its misalignment.

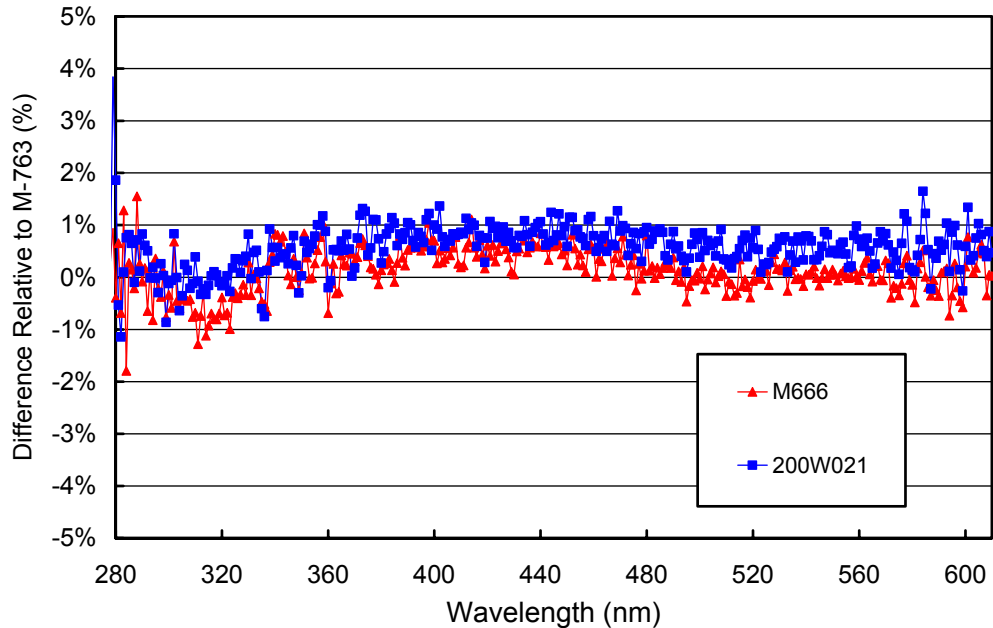


Figure 5.3.3. Comparison of South Pole lamps 200W021, and M-666 with BSI traveling standard M-763 at the beginning of the Volume 18 season (1/23/08–1/24/08). Data of lamp M-763 have been corrected for the effect of its misalignment.

5.3.2. Instrument Stability

The stability of the spectroradiometer's sensitivity over time is primarily monitored with bi-weekly calibrations utilizing the on-site standards and daily response scans of the internal irradiance reference lamp. The stability of the internal lamp is monitored with the TSI sensor, which is independent from possible monochromator and PMT drifts.

Figure 5.3.4 shows changes in TSI readings and PMT currents at 300 and 400 nm, derived from the daily scans of the internal lamp during the South Pole 2007/08 season. The TSI measurements indicate that the internal lamp became dimmer by about 2% during this period. This amount of drift is typical. The PMT currents at 300 and 400 nm varied by about $\pm 2\%$, indicating good stability of the instrument.

Absolute calibrations indicated some variation of the system responsivity, which were mostly related to transmission changes of the irradiance collector due to ice-buildup underneath the cosine diffuser. To correct for these changes, five different calibration functions were applied to solar measurements of Volume 17. An overview of calibration periods is provided in Table 5.3.1. Figure 5.3.5 shows ratios of all calibration functions relative to the function applied during Period P1. Note that this period covers the entire period up to the onset of winter darkness. During the Polar Night, ice formed underneath the cosine collector, which explains the difference of 4-5% between Periods P1 and P2. Removal of the ice changed the responsivity by about 6% (difference between periods P2 and P3).

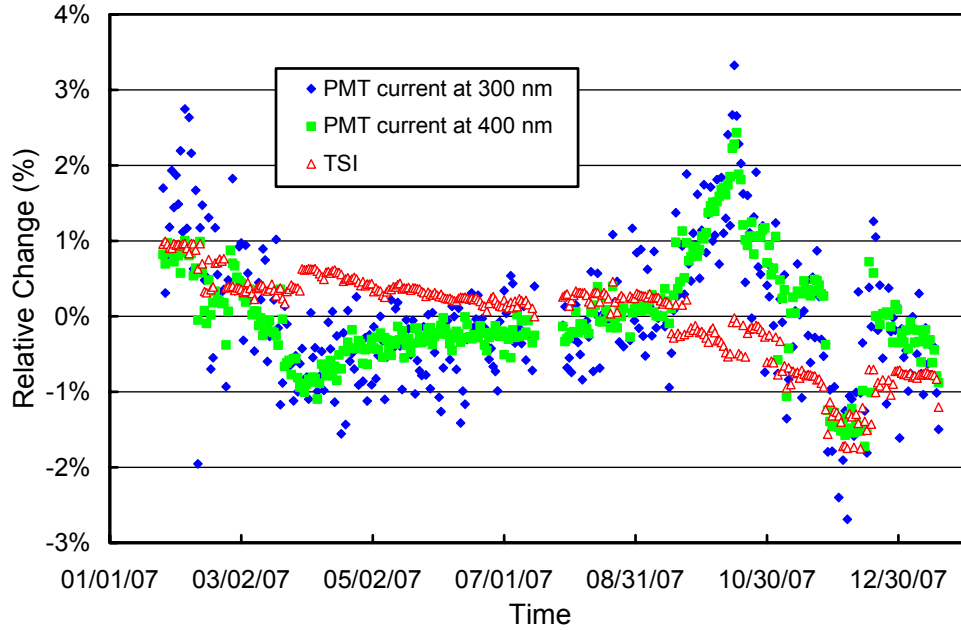


Figure 5.3.4. Time-series of PMT current at 300 and 400 nm, and TSI signal for measurements of the internal irradiance standard performed during the South Pole 2007/08 season. Data are normalized to the average of the whole period.

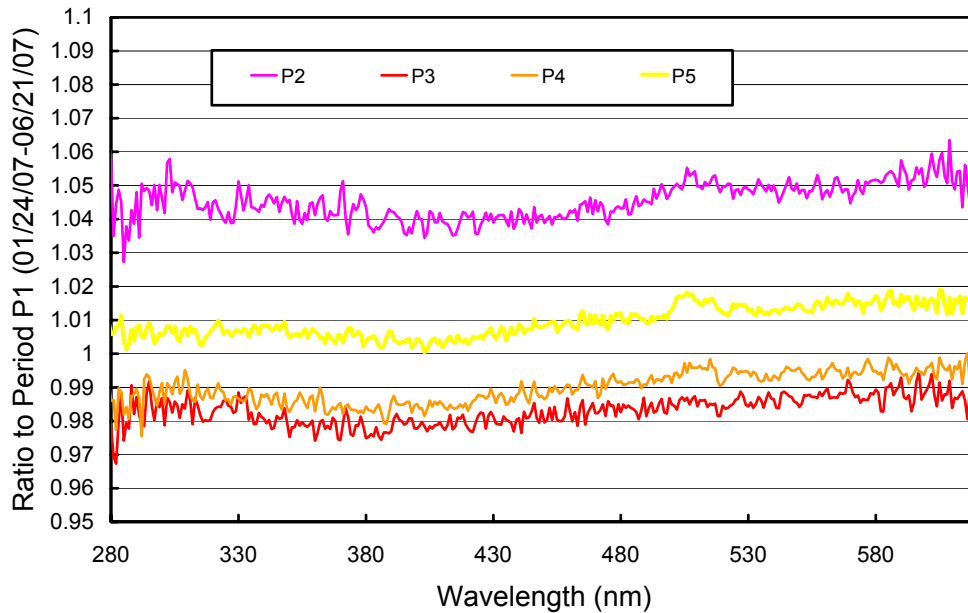


Figure 5.3.5. Ratios of irradiance assigned to the internal lamp relative to Period P1.

Figure 5.3.6 presents the relative standard deviation calculated from the individual calibration scans of each period. These data are useful for estimating the variability of calibrations in each period. The

variability is typically less than 1.5% for wavelengths above 300 nm, indicating very good stability for all periods.

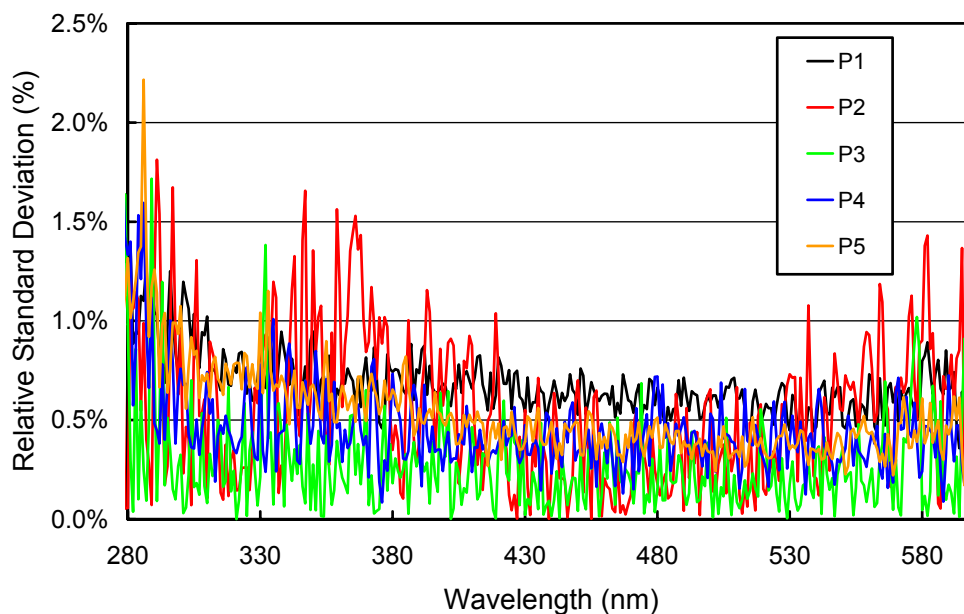


Figure 5.3.6. Relative standard deviation calculated from the absolute calibration scans measured during the South Pole 2007/08 season.

Table 5.3.1: Calibration periods for South Pole Volume 17 data.

Period name	Period range	Number of Absolute Scans	Remarks
P1	01/25/2007 – 06/21/2007	10	Before Polar Night
P2	06/22/2007 – 10/09/2007	3	After Polar Night
P3	10/10/2007 – 10/18/2007	3	Collector cleaning before period
P4	10/19/2007 – 11/23/2007	2	
P5	11/24/2007 – 01/18/2008	8	

5.3.3. Wavelength Calibration

Wavelength stability of the system was monitored with the internal mercury lamp. Information from the daily wavelength scans was used to homogenize the data set by correcting day-to-day fluctuations in the wavelength offset. Figure 5.3.7 shows the difference of the wavelength offset of the 296.73 nm mercury line between two consecutive wavelength scans. A total of 403 pairs of scans were evaluated. The change in offset was less than ± 0.025 nm for 98% of the scans and smaller than ± 0.055 nm for 99% of the scans. Only the shift of one scan-pair was larger than ± 0.1 nm, which was caused by operator intervention. The wavelength calibration was adjusted accordingly.

After data were corrected for day-to-day wavelength fluctuations, the wavelength-dependent bias between this homogenized data set and the correct wavelength scale was determined with the Version 2 Fraunhofer-line correlation method (Bernhard *et al.*, 2004). Analysis indicated that the monochromator's wavelength mapping had slightly changed during the polar night. Two calibration functions were established and are shown in Figure 5.3.8. One was applied up to April 2007 (Function A), and one for period following the months of winter darkness (Function B). The functions exceed 1 nm for wavelengths larger than 500 nm.

The magnitude of the correction is considerably larger than for other sites and caused by the properties of the monochromator installed. The accuracy of solar data is not compromised since the correction is well defined.

After data had been wavelength-corrected using the shift-functions described above, the wavelength accuracy was tested again with the Version 2 Fraunhofer-line correlation method. The results are shown in Figure 5.3.9 for four UV wavelengths. The standard deviation of the residual shifts is less than 0.02 nm. The actual wavelength uncertainty of the instrument may be slightly larger as indicated in Figure 5.3.9 due to wavelength fluctuations during a given day (Figure 5.3.9 shows only one point per day), and possible systematic errors of the Fraunhofer-correlation method (*Bernhard et al.*, 2004).

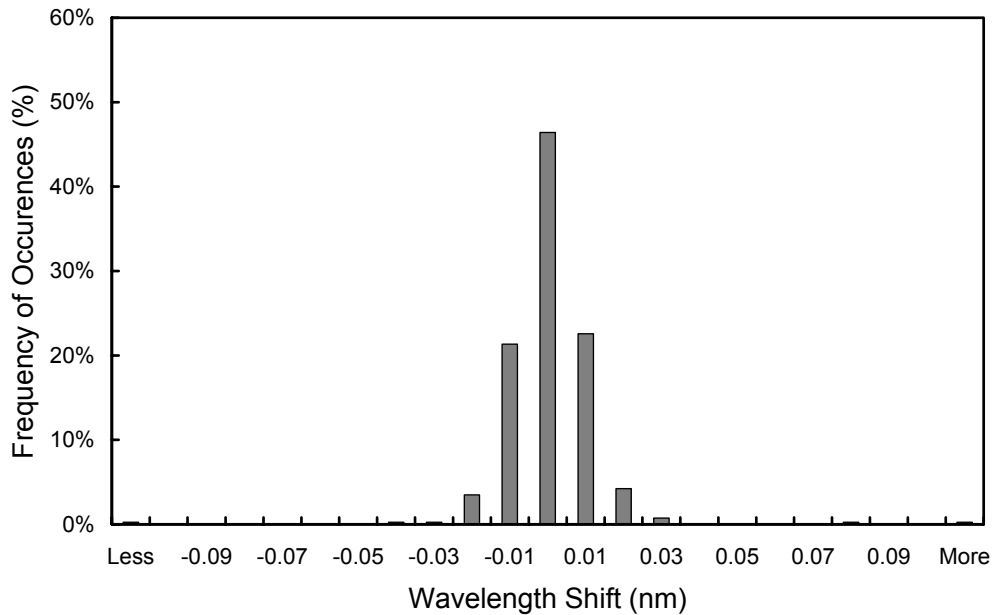


Figure 5.3.7. Frequency distribution of the difference of the measured position of the 296.73 nm mercury line between consecutive wavelength scans. The x-labels give the center wavelength shift for each column. The 0-nm histogram column covers the range -0.005 to +0.005 nm. “Less” means shifts beyond -0.105 nm; “more” means shifts beyond +0.105 nm.

Data from the external mercury scans do not have a direct influence on data products but are an important part of instrument characterization. Figure 5.3.10 illustrates the difference between internal and external mercury scans collected during system service in 2007 and 2008. Measurements of the two years are consistent. The wavelength scale of the figure is the same as applied during solar measurements. The peak of the external scans agrees well with the nominal wavelength of 296.73 nm, whereas the peak of the internal scans is shifted about 0.10 nm to shorter wavelengths. External scans have a bandwidth of about 1.04 nm FWHM. The bandwidth of the internal scan is 0.73 nm. External scans have the same light path as solar measurements and therefore represent the monochromator’s bandpass relevant for solar scans.

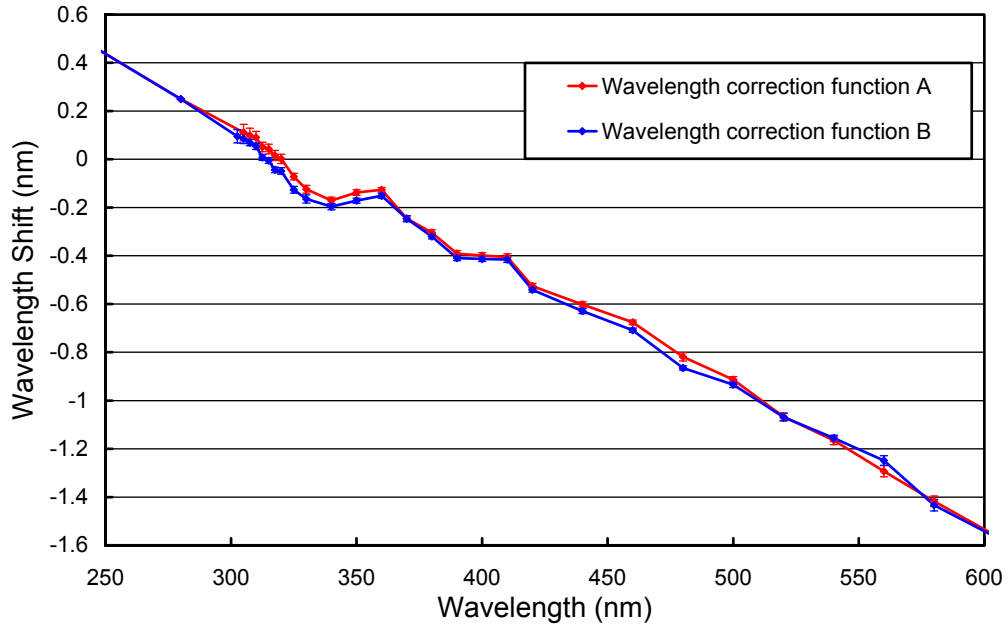


Figure 5.3.8. Monochromator non-linearity correction function for the South Pole 2007/08 season.

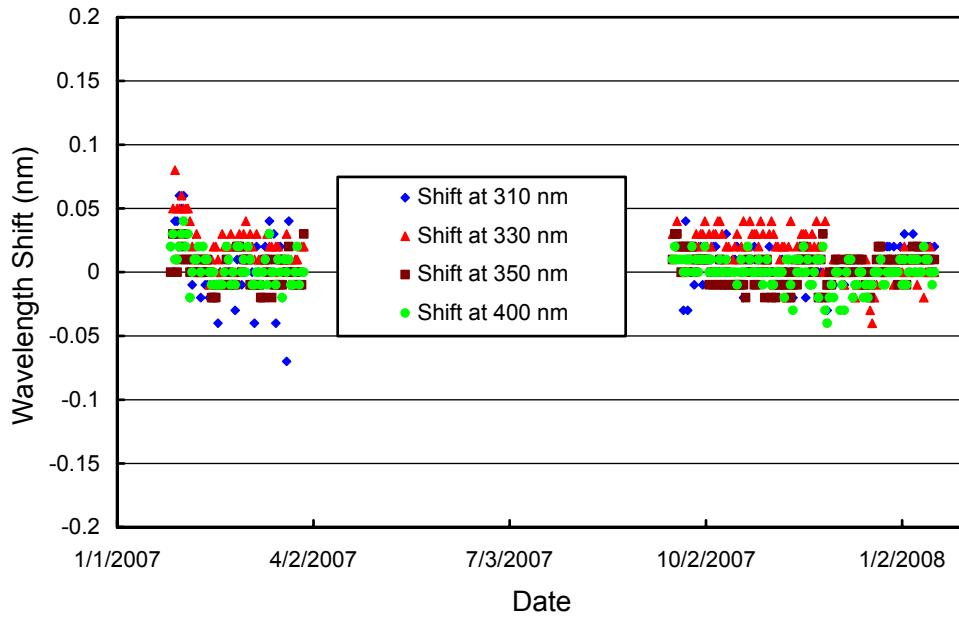


Figure 5.3.9. Wavelength accuracy check of final data at four wavelengths by means of Fraunhofer-line correlation. Measurement performed at 00:00 UT were evaluated for each day of the season. No data exist during Polar Night.

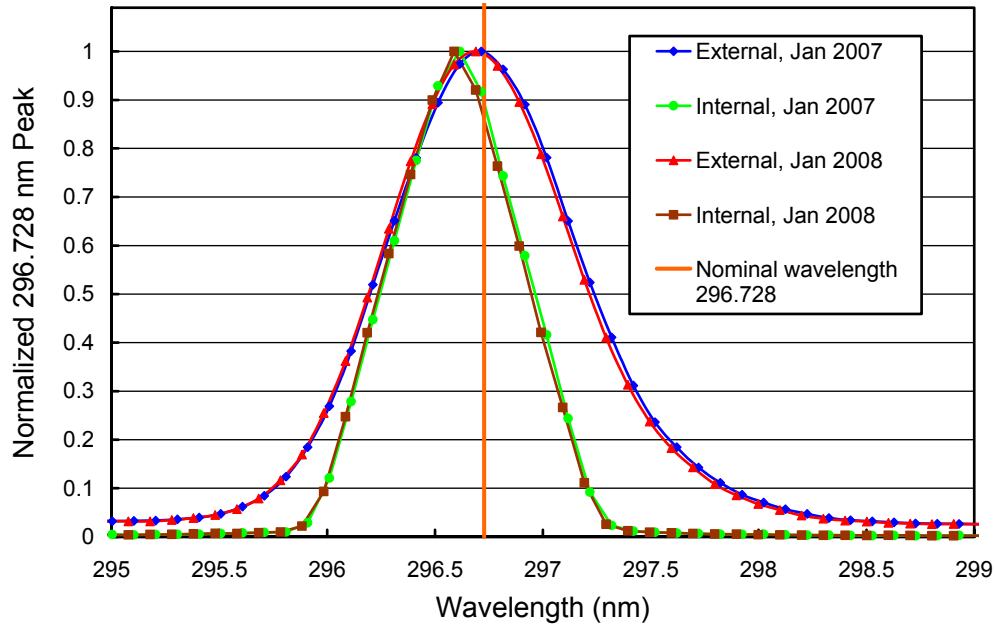


Figure 5.3.10. The 296.73 mercury line as registered by the PMT from external and internal sources.

5.3.4. Missing Data

A total of 16995 scans are part of the South Pole Volume 17 dataset. These are about 95% of the maximum possible number of data scans. 901 solar scans were superseded by calibration scans. Since South Pole Station has 24 hours of sunlight per day during the summer season, a loss of solar data cannot be avoided. Only 8 scans were missed due to technical problems. A break-down of missing data is provided in Table 5.3.2

Table 5.3.2. Missing solar scans in the South Pole Volume 17 data set.

Period	Number of scans	Reason
<i>Calibration scans</i>		
Throughout season	345	Response scans
Throughout season	423	Wavelength scans
Throughout season	129	Absolute scans
<i>Technical problems</i>		
02/02/07	2	Survey of collector position with GPS
02/12/07	8	Exchange and characterization of Eppley PSP pyranometer
10/09/07	4	Cleaning of ice build-up underneath collector
<i>Other</i>		
Throughout season	29	Collector shaded by nearby obstacles, e.g. air sampling stack

5.3.5. GUv Data

The GUv-541 radiometer, which is installed next to the SUV-100, was calibrated against final SUV-100 measurements following the procedure outlined in Section 4.3.1. The calibration of the instrument's 305, 313, and 320 nm channels drifted by 6%, 5%, and 14%, respectively, over the course of the year. Drifts of the 340 and 380 nm channels were smaller than 2.5%. To corrected for these changes, the GUv time-series was broken into four periods and different calibration factors were applied for these periods. Drifts in published GUv data are smaller than 3%.

Data products were calculated from the calibrated measurements (Section 4.3.2). Figure 5.3.11. shows a comparison of GUv-541 and SUV-100 erythemal irradiance based on final Volume 17 data. For solar zenith angles smaller than 80°, measurements of the two instruments agree to within $\pm 3.6\%$ ($\pm 1\sigma$), except for times when an air sampling stack installed at the ARO building casts a shadow on the GUv-541 radiometer but not on the SUV-100.⁺ We advise data users to use SUV-100 rather than GUv-541 data whenever possible, in particular for low-Sun conditions.

Figure 5.3.12 shows a comparison of total ozone measured by the GUv-541 radiometer, the SUV-100 (Version 2 data set; see www.biospherical.com/NSF/Version2), and the Ozone Monitoring Instrument (OMI) installed on NASA's AURA satellite. GUv-541 ozone values were calculated as described in Section 4.3.3. There is good agreement between the three data sets between October and December. Between January and March 2007, SUV-100 measurements are on average 3% larger than OMI observations. The ratio of GUv-541 / OMI decreases between January and March 2007. A similar bias has been observed also in previous years. The reason of this systematic change is caused by the choice of the ozone profile used in by the inversion method, which is optimized for the austral spring. GUv-541 ozone data become unreliable for SZA larger than 80° and should not be used.

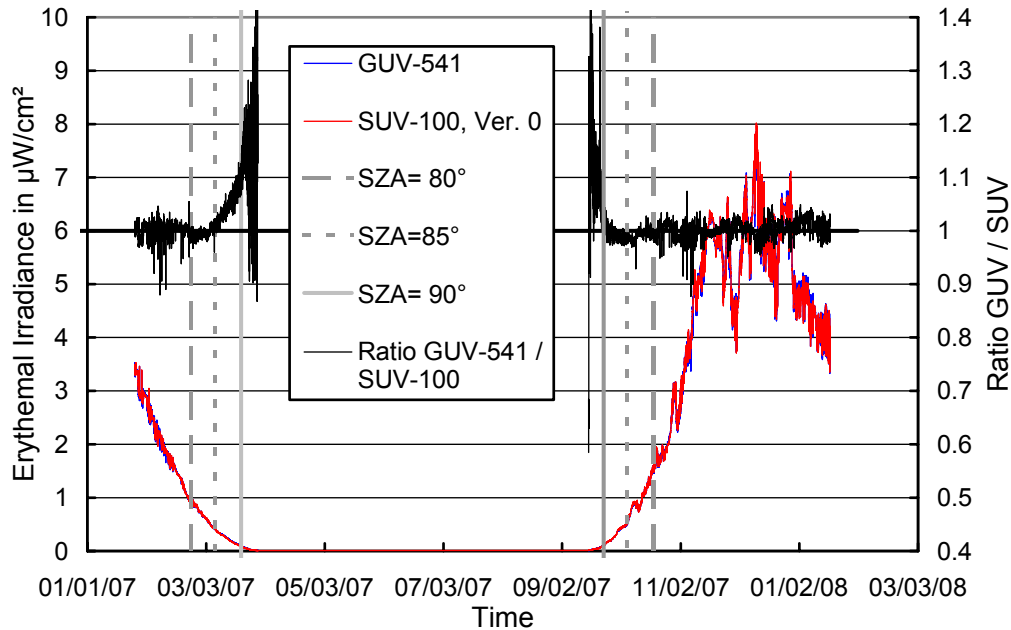


Figure 5.3.11. Comparison of erythemal irradiance measured by the SUV-100 spectroradiometer and the GUv-541 radiometer. SUV-100 measurements are based on “Version 0” (cosine-error uncorrected) data.

⁺ SUV-100 data affected by shading from the air sampling stack have been excluded from the published data set. GUv-541 data concurrent with shaded SUV-100 measurements have also been excluded. Since the SUV-100 collector is located approximately 2 meters away from the GUv-541 radiometer, both instruments are not shaded during exactly the same time and some data affected by the stack are still part of the GUv-541 data set.

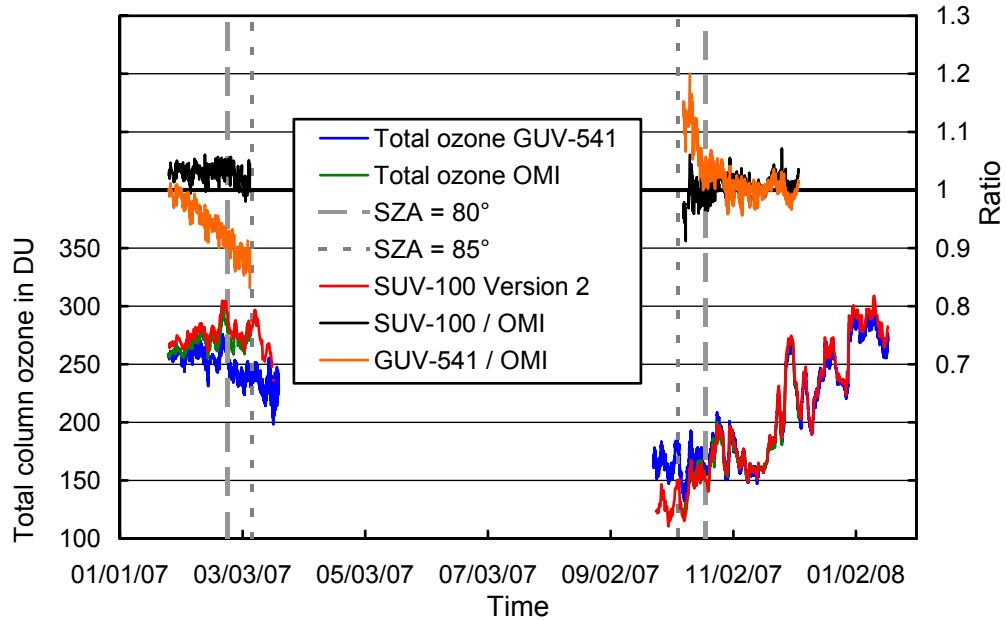


Figure 5.3.12. Comparison of total column ozone measurements from GUV-541, SUV-100 (Version 2 data), and OMI. GUV-541 and SUV-100 measurements are plotted in 15 minute intervals. For calculating ratios of data sets, only GUV-541 and SUV-100 measurements concurrent with OMI overpass data were evaluated. OMI data measured after 4 December 2007 were not available as of this writing.